


Fluidity and Hot Cracking Susceptibility of A356 Alloys with Sc Additions

K. Puparattanapong¹ · P. Pandee¹ · S. Boontein¹ · C. Limmaneevichitr¹ 

Received: 15 September 2017 / Accepted: 30 January 2018 / Published online: 23 February 2018
© The Indian Institute of Metals - IIM 2018

Abstract A356 with scandium (Sc) addition provides interesting results beyond costs. For the practical use of Sc, the effects of Sc on castability must be considered. Fluidity and hot cracking are important factors defining the castability of aluminum casting alloys. In the present work, the influence of Sc addition on the castability of A356 hypoeutectic Al–Si alloy was investigated, which was evaluated through fluidity and hot cracking susceptibility. The fluidity of the alloys was studied by measuring the total volume of solidified aluminum in a multi-channel mold. The hot cracking susceptibility of the alloys was evaluated by using a constrained-rod casting mold test. The results of the fluidity and hot cracking susceptibility test were supported by microstructural analysis. The results indicate that 0.2 wt% Sc addition significantly increases the fluidity of A356 alloy, due to the grain refinement and eutectic Si modification by changing the solidification mode. However, the fluidity slightly decreases when the Sc content increases to 0.4 wt% due to the formation of primary Al₂Si₂Sc intermetallic phase. The hot cracking of A356 alloy was completely diminished when Sc was added to the alloy.

Keywords Aluminum alloy · Castability · Grain refinement · Modification · Scandium

1 Introduction

The castability of an alloy plays a key role for foundry industries as it affects the quality and soundness of the casting products. Two of the important castabilities included in this work are fluidity and hot cracking susceptibility. The fluidity limits the castability of alloys and their final properties, e.g., surface finish and minimum wall thickness. The fluidity is typically defined as the length of the metal flowing in a channel with a small cross-sectional area while solidifying [1, 2]. Hot cracking or hot tearing is a common and severe defect that occurs during solidification in aluminum alloy castings. The formation of hot cracking is normally linked to insufficient melt feeding of solidification shrinkage and thermal accumulation induced stresses during solidification contraction. The hot cracking occurs when the stress level exceeds the strength of the mushy and not enough liquid metal is available to fill [1, 3, 4]. Alloying addition is one of the major factors that have influences on the fluidity and hot cracking of aluminum alloy castings [1, 5].

Many researchers have investigated the relationship between grain refinement and fluidity. However, the effect of grain refinement on fluidity is still unclear. Grain refinement has often been reported to increase the fluidity of aluminum alloy. It has been reported that the addition of Al–5Ti–1B grain refiner into A356 alloy have resulted in increased fluidity of the alloy [6, 7]. Some authors have argued that grain refinement with grain refiners containing Ti reduces the fluidity of aluminum alloy castings [8, 9]. Similarly, there is no consensus on the effect of modifiers such as Sr and Na elements on fluidity. Kotte [10] reported that both Sr and Na modifications reduces fluidity. Contrary to the abovementioned findings, the addition of Sr modifier has been reported to increase the fluidity of alloy

✉ C. Limmaneevichitr
chaowalit.lim@mail.kmutt.ac.th

¹ Department of Production Engineering, Faculty of Engineering, King Mongkut's University of Technology Thonburi, 126 Pracha-Utid Rd., Bangmod, Tungkhru, Bangkok 10140, Thailand

[11]. Moreover, other reports indicated that Sr and Na modifiers does not significantly change the fluidity [12].

Many investigations have been conducted on the effects of grain refinement on hot cracking. However, the results are not consistent and are sometimes confusing. Easton et al. [13] studied the effect of Ti addition on hot cracking of aluminum alloy by measuring the load development in the solidifying test bar. It has been concluded that grain refinement decreases the hot cracking susceptibility through changing the grain morphology from columnar to equiaxed and reducing the grain size. However, Rosenberg et al. [14] suggested that grain refinement does not have any effect on hot cracking in their experiment. Furthermore, Warrington et al. [15] found that the alloy can still have high hot cracking susceptibility even when a grain refiner is added, depending on the amount of grain refiner addition.

A356 aluminum alloy is extensively used in many applications such as wheel rims and automotive engine parts, aerospace aircraft fittings and control parts, aircraft pump components. Its attractiveness is due to excellent castability, high strength-to-weight ratio, and good corrosion resistance [16, 17]. The mechanical properties attainable in this alloy are controlled by the microstructure of the alloys.

The well-known positive effects of Sc addition into aluminum alloys have made it a promising candidate as a chemical modifier in hypoeutectic Al–Si casting alloys. There have been recent studies indicating that the addition of 0.2–0.4 wt% Sc in hypoeutectic Al–Si casting alloy have many benefits, i.e., refinement of α -Al dendrite grain and secondary dendrite arm spacing (SDAS) [18–21], modification of eutectic Si from a coarse plate-like structure to a fibrous structure [22, 23], and changing of iron-rich intermetallic phase from needle-like (β -phase) into Chinese script-like (α -phase), which reduces the harmful effects of β -phase [24]. Additionally, from a previous work [25], it has been found that Sc additions into A356 alloys have resulted in decreased sizes and more dispersed porosities across the samples.

Prior to the practical implementation of Sc as an alloying element for aluminum alloy casting, there are many factors that need to be studied, especially the castability. In a previous work [25], the effect of Sc on the porosity formation of A356 alloy, i.e., one of the castability phenomena, has been investigated. Prukkanon et al. [26] presented the results of the effect of Sc on the fluidity of A356 alloy by using a vacuum test. However, the fluidity test by using a vacuum did not resemble the practical casting. Moreover, we have not found any work on the influence of Sc on hot cracking susceptibility. Thus, the objective of the present study is to investigate the influence of Sc additions on the castability, i.e., fluidity, by using a

multi-channel mold and hot cracking susceptibility of hypoeutectic Al–Si alloys.

2 Experimental Procedure

2.1 Alloying and Casting

The A356 aluminum ingots with the approximate dimensions of $60 \times 630 \times 35 \text{ mm}^3$ used in this work were made from primary aluminum to minimize any possible contamination effects by trace elements. Individual ingot weight was about 4 kg. These ingots were also prepared from the same batch to minimize any undesired variations. A master alloy of Al–2 wt% Sc was used to add minor Sc to obtain various chemical compositions. The A356 based alloy was melted in a silicon carbide crucible in a 12-kW induction furnace. The melt was heated up to 800 °C before the addition of Al–2 wt% Sc master alloy to obtain the target compositions in each batch. Each molten alloy taken from crucible was cast in a copper mold to obtain a disk-shaped sample for chemical analysis by a spark emission spectrometer. The chemical compositions are shown in Table 1 (along with the alloy designations). After the adjustment of chemical compositions, covering and cleaning flux were used by approximately 0.5 wt% of the alloy. The melt was degassed by purging argon through a stainless-steel tube (6-mm inside diameter) with a flow rate of 4 L/min at a pressure of 0.2 MPa for approximately 1 min in each experiment. The melt was then carefully skimmed to remove dross and other impurities.

2.2 Fluidity Test

The fluidity test was done by using a multi-channel mold, as illustrated in Fig. 1a. The mold design with multi-channel difference in thickness was successfully used in previous works [27, 28]. The mold was made from steel with five channels of different thicknesses. The cross section of the channel was rectangular. Each channel was 295 mm long and 15 mm wide, and the thickness of the channel was either 2, 3, 5, 7, or 9 mm. The multi-channel mold was pre-heated to 300 °C using a heater rod with digital temperature controller. In addition, for better control of the pouring height and pouring rate, a specially designed mechanism was installed for the steel pouring cup and a plug, which was preheated in a separate resistance furnace at 650 °C. Approximately 695 g of molten aluminum was poured into the pouring cup. The temperature of the melt was measured using a K-type thermocouple to ensure that the pouring temperature was stable at 750 °C for all experiments. The experimental set up of the fluidity test is shown in Fig. 2a. The fluidity was obtained by measuring

Table 1 Chemical composition of the samples, as determined by emission spectrometry

Composition	Element (wt%)				
	Si	Mg	Fe	Sc	Al
Unmodified A356	7.32	0.31	0.15	Nil	Balance
A356 + 0.2 wt% Sc	7.03	0.28	0.13	0.19	Balance
A356 + 0.4 wt% Sc	7.25	0.21	0.13	0.36	Balance

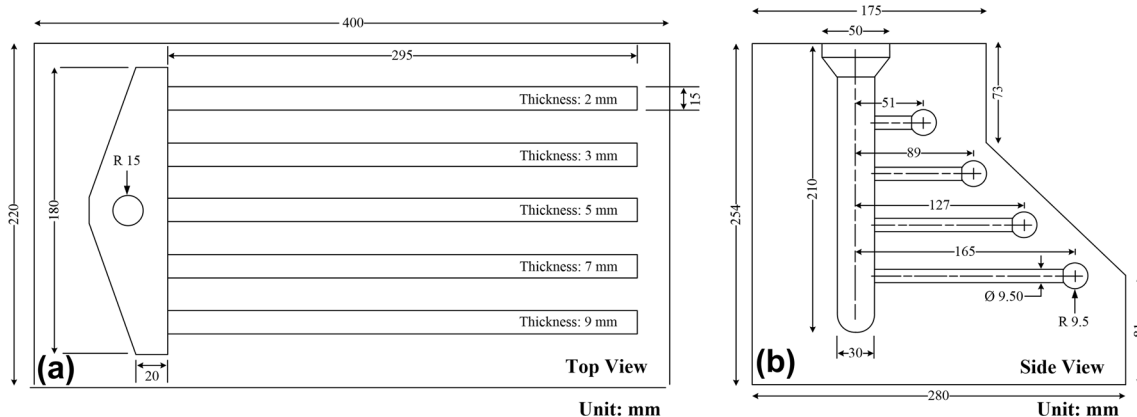


Fig. 1 Illustrations of **a** the fluidity test mold, and **b** the hot cracking susceptibility test mold

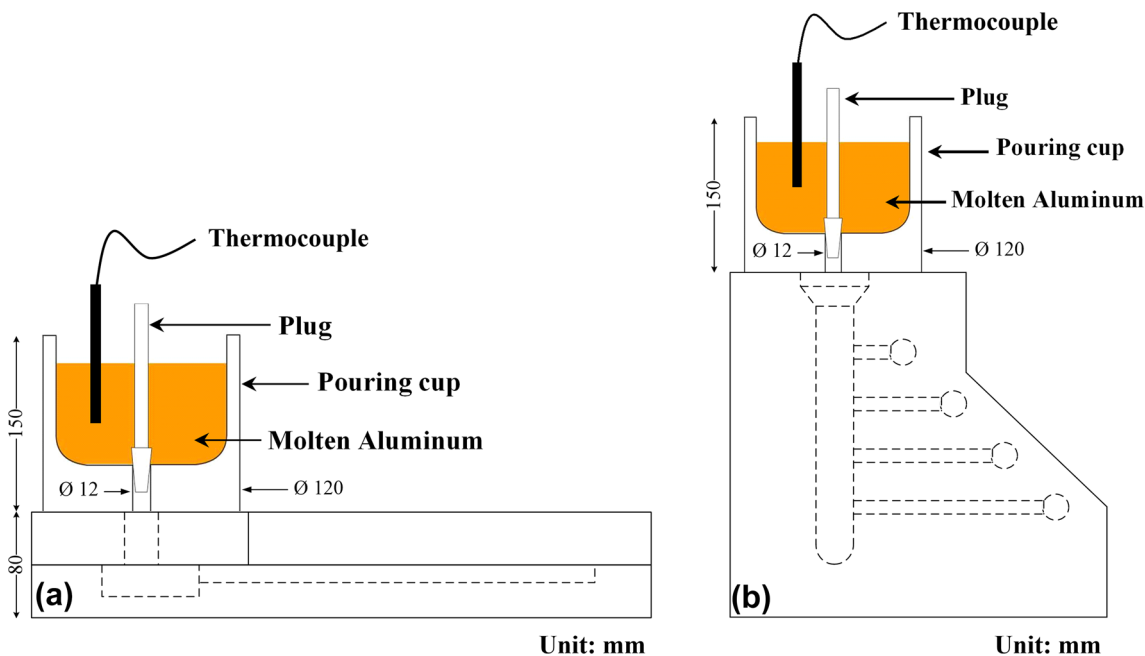


Fig. 2 Experimental setups for **a** the fluidity test, and **b** the hot cracking susceptibility test

the total volume of the solidified sample. The total volume in the five channels has been calculated as follows [27]:

$$V = \sum_{i=1}^5 A_i \times L_i \tag{1}$$

In Eq. 1, V is the total volume, A_i is the cross-sectional area, and L_i is the length of each strip. The total volume of the solidified sample was measured from five tests for each set of alloys. The results were averaged, and the standard deviations were calculated.

2.3 Hot Cracking Test

The hot cracking was done by using a constrained-rod casting (CRC) mold test developed by Pekguleryuz et al. [29], as shown in Fig. 1b. The mold consisted of four rods all with a diameter of 9.5 mm and with varying lengths of 51, 89, 127, and 165 mm. The rods were constrained at one end by the sprue and were contained at the other end with a ball of 19 mm diameter that acted as an anchor to restrain the rod from free contraction during casting. The CRC mold was preheated to 200 °C, and then approximately 500 g of the molten aluminum was poured into the pouring cup. The temperatures of the melt were measured using a K-type thermocouple to ensure that the pouring temperatures were stable at either 750, 775 or 800 °C. The experimental set up of the hot cracking susceptibility test is shown in Fig. 2b. The hot cracking susceptibility (HCS) is defined as follows [30]:

$$HCS = \sum w_{crack} \times f_{length} \times f_{location} \quad (2)$$

In Eq. 2, w_{crack} is the maximum crack width measured in mm, f_{length} is the value of the rod length factor, which is 4 for the longest rod, 8 for the second longest rod, 16 for the third longest rod, and 32 for the shortest rod, and $f_{location}$ is the value of the crack location factor, which is 1 for cracking at the sprue end, 2 at the ball end and 3 in the middle of the rod. The determinations of the rod length factor and the crack location factor are shown in Fig. 3.

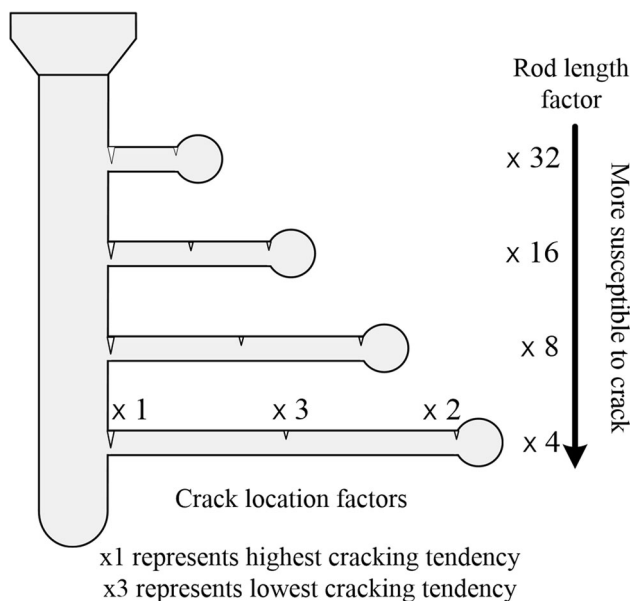


Fig. 3 Determining crack sensitivity from widths of cracks in CRC: rod length factor and crack location factor

2.4 Microstructural Observation

All optical/SEM/BSE micrographs were analyzed on samples taken from the areas near an ingate of 9-mm thick channel of the fluidity test mold, which have a large enough area and complete availability for all sample preparations. The obtained samples were subsequently prepared by standard metallographic procedures with a final polishing by a 0.05 μm colloidal silica suspension. The samples were then etched with 0.5% HF-water solution. The microstructures from all samples were observed using an optical microscope (OM) and scanning electron microscope (SEM) equipped with an energy-dispersive X-ray spectroscopy (EDS) detector and equipped with EDAX_TSL EBSD hardware, together with the OIM_TSL Collection 5.3 software for automated recognition and indexing of electron backscatter diffraction analysis (EBSD). Moreover, the samples were etched in Tucker's reagent (45 ml HCl, 15 ml HNO₃, 15 ml HF, 25 ml H₂O) to highlight the grain boundaries, and then grain sizes were measured by the linear intercept method with iSolution DT image analysis software.

3 Results

A comparison of the average total volume of the various alloys is shown in Fig. 4. It can be observed in Fig. 4 that the first addition of 0.2 wt% Sc significantly improves the average total volume of the solidified alloy compared to the A356 based alloy, and that further increase in the Sc content (0.4 wt%) slightly deteriorates the total fluidity length and total volume of the solidified alloy. The best fluidity is 90,216 mm³ (0.2 wt% Sc) where the average total volume improves by 8.66% compared with the A356 base alloy.

Optical macrographs taken from the cross section of the fluidity samples of A356 alloys without and with Sc additions are shown in Fig. 5. Sc addition can significantly reduce grain size in Al–Si alloys [21, 26]. In this study, we have also found that the addition of 0.2 and 0.4 wt% Sc reduces the grain size from 823 to 447 μm and to 490 μm , respectively, as shown in Fig. 5a–c. Optical micrographs at low magnification of the A356 based alloy (Fig. 5d) contains coarse α -Al dendrite structures. The addition of Sc changes this coarse α -Al dendrite structure to a finer dendrites structure and more equiaxed structure as shown in Fig. 5e, f. At high magnification, the A356 based alloy (Fig. 5g) exhibits coarse plate-like eutectic Si morphology. It can be seen that Sc alters the coarse plate-like morphology to a fine fibrous eutectic Si morphology, as shown in Fig. 5h, i. Thus, Sc refines the α -Al grain structure and modifies the eutectic Si.

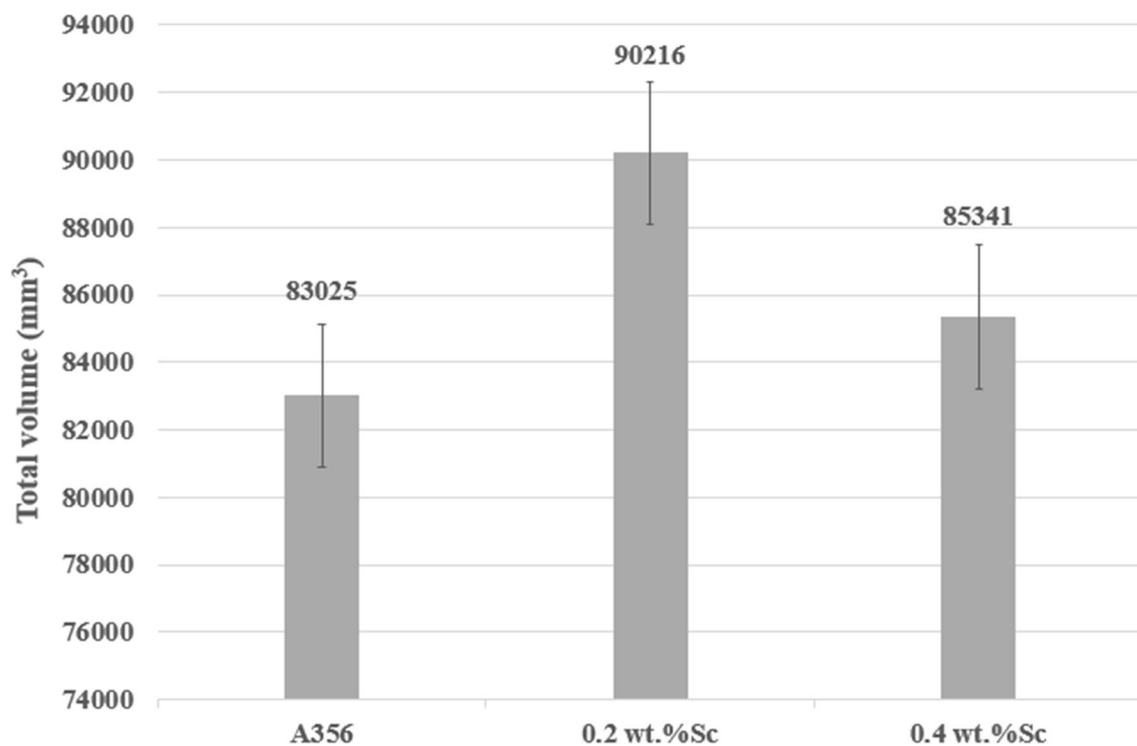


Fig. 4 Total volume of fluidity samples

BSE micrographs of the fluidity samples of A356 alloy with 0.2 and 0.4 wt% Sc addition are shown in Fig. 6a, b, respectively. It can be seen from Fig. 6a that the addition of 0.2 wt% Sc contributes to the formation of an intermetallic phase in the eutectic region. The addition of 0.4 wt% Sc further increases the amount of intermetallic phase (Fig. 6b). Figure 7 shows SEM analysis of a eutectic region in the 0.4 wt% Sc sample. The SE image in Fig. 7a shows that the eutectic structure contains the intermetallic phase. To identify the intermetallic phase, EDS mapping and EDS point analysis have been performed on the intermetallic particle, as shown in Fig. 7b–e. As shown in the EDS analysis, the intermetallic particle contains Al, Si, and Sc. Note that this intermetallic phase is a phase in the Al–Si–Sc system [31, 32]. Figure 8 shows the optical micrograph of the 0.4 wt% Sc sample. The micrograph shows that the intermetallic phase is on the aluminum dendrite. EBSD analysis has been carried out to confirm the EDS results and to identify the Sc-containing intermetallic phase in the Sc added samples, which is shown in Fig. 9. Figure 9a is the Kikuchi pattern of the Sc-containing intermetallic phase. Figure 9b is the pattern indexed as tetragonal AlSi_2Sc_2 with the $tP10\text{-Si}_2\text{U}_3$ -type structure determined by Tyvanchuk et al. [33]. By combining the EDS and EBSD results, it can be confirmed that the Sc-containing phase is AlSi_2Sc_2 (τ phase).

The hot cracking susceptibility indexes of A356 based alloys with pouring temperatures of 750, 775, and 800 °C

are 12.46, 12.70, and 12.71, respectively. The hot cracking does not occur at all in the A356 alloys with Sc additions. The macrograph and SEM micrograph of the hot cracking surfaces of the A356 based alloy are shown in Fig. 10a, b, respectively. The SEM micrograph exhibits that the hot cracking of the A356 alloy apparently propagates through the dendrite structure.

4 Discussion

4.1 Fluidity

Grain refinement is one of the major factors influencing the fluidity of an alloy. Many studies have reported the relationship between fluidity and grain size. Dahle et al. [7] observed a variation in fluidity with Al–5Ti–1B addition in A356 alloy. They found that the fluidity was reduced with Ti addition below 0.12 wt%, while the fluidity was increased with Ti additions above 0.12 wt%. Kwon et al. [6] reported that the addition of Ti and Al–5Ti–1B significantly increased the fluidity of A356 alloy.

The results in Fig. 4 show that the addition of 0.2 wt% Sc increases the fluidity of the A356 alloy, due to the α -Al grain refinement, as shown in Fig. 5. The results are similar to a previous work by Prukkanon et al. [26]. It is also found that the addition of Sc to hypoeutectic Al–Si alloy significantly reduces the α -Al grain size and increases the

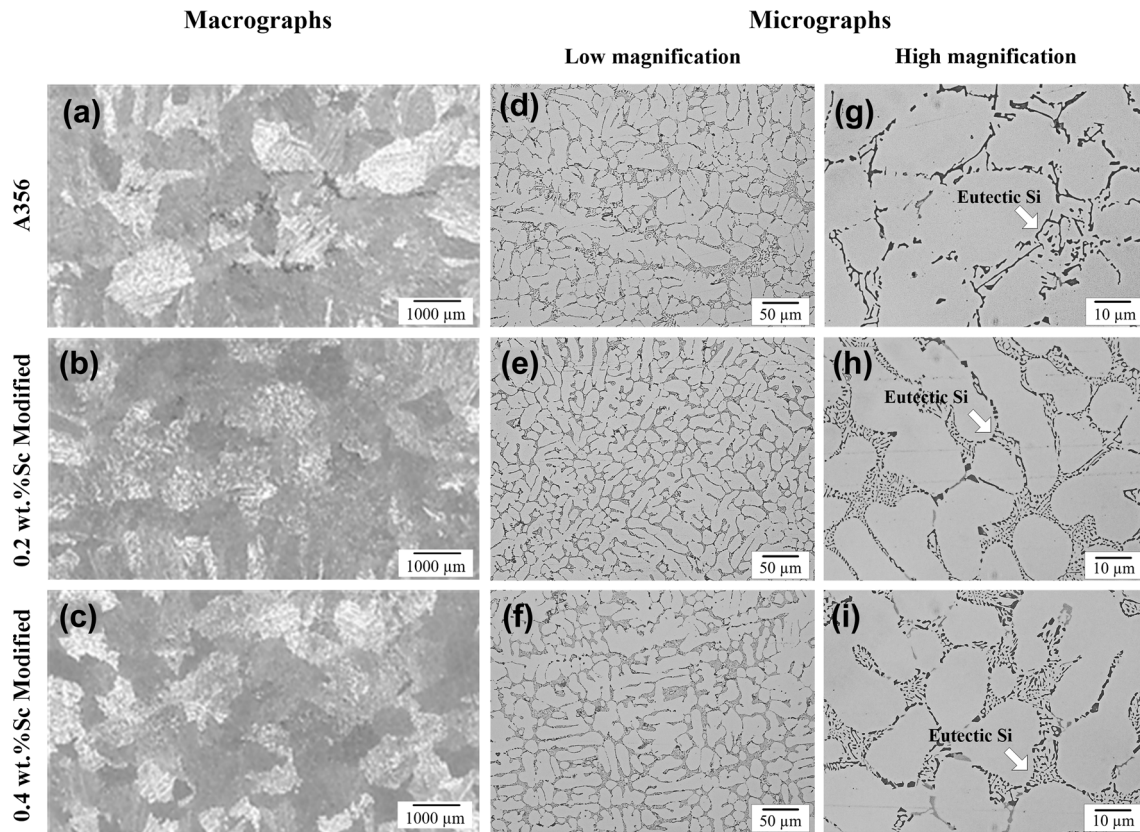


Fig. 5 Optical macrographs and micrographs taken from the cross-section of the fluidity samples of A356 alloys without and with Sc additions. Macrographs of **a** A356, **b** 0.2 wt% Sc, and **c** 0.4 wt% Sc. Micrographs at low magnification **d** A356, **e** 0.2 wt% Sc, and **f** 0.4 wt% Sc. Micrographs at high magnification **g** A356, **h** 0.2 wt% Sc, and **i** 0.4 wt% Sc

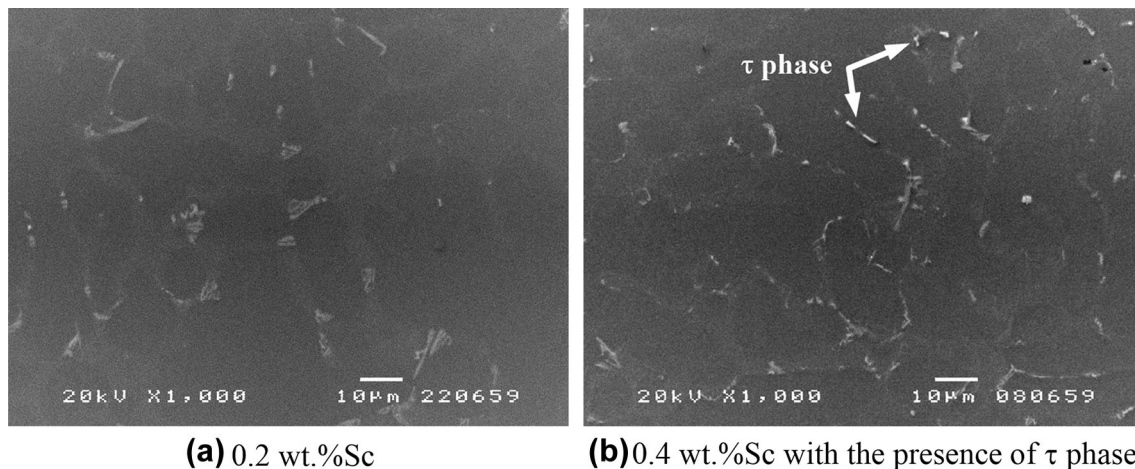


Fig. 6 BSE micrographs of **a** 0.2 wt% Sc alloy, and **b** 0.4 wt% Sc alloy with the presence of τ phase

fluidity in the vacuum fluidity test. In this study, with the addition of 0.2 wt% Sc in A356 alloy, the grains are remarkably refined. Therefore, it can be concluded that the significant improvement of fluidity is closely related to the refinement of grains.

There are general explanations for the relationship between fluidity and grain refinement in terms of dendrite coherency point. The dendrite coherency point is referred to as the point where individual dendrites first impinge upon their neighbors in the solidification process of the

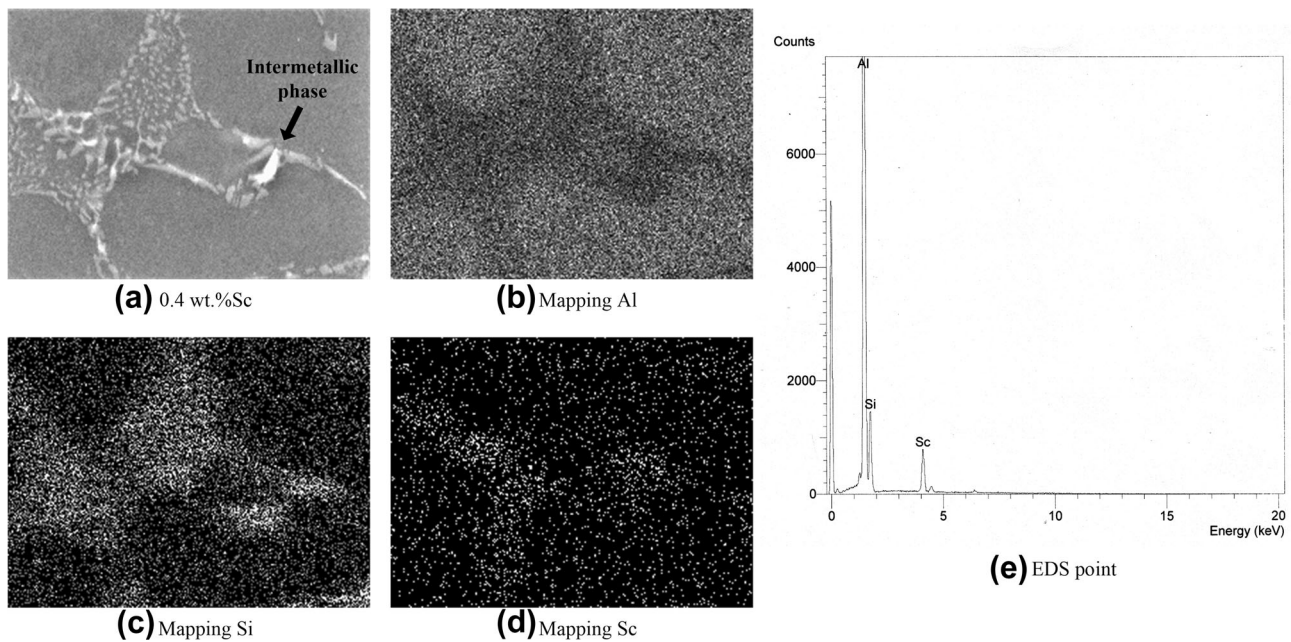


Fig. 7 SE micrographs and EDS analysis of the AlSi_2Sc_2 phase in eutectic region: **a** SE image, EDS mapping, **b** Al, **c** Si, and **d** Sc and **e** EDS point

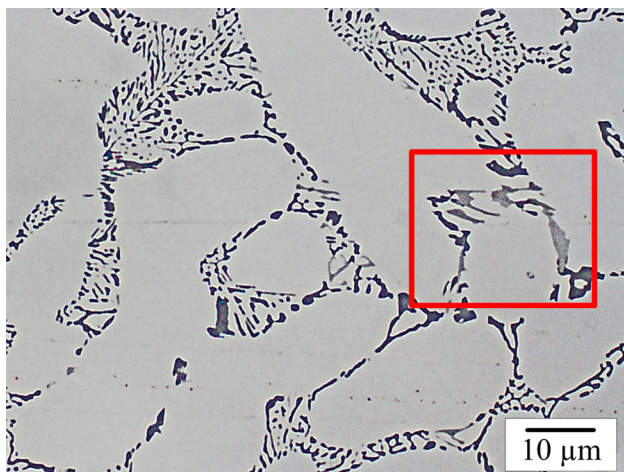


Fig. 8 Optical micrograph of 0.4 wt% Sc sample

alloy [34]. Malekan et al. [35] reported that the addition of Al–5Ti–1B grain refiner can increase the temperature interval of coherency, coherency fraction solid, and coherency time. Grain refinement postpones the dendrite coherency, so dendrites become coherent later. Thus, late dendrite coherency allows more time for fluid flow and hence increases the fluidity. However, the effect of grain refinement on the fluidity of Al-based alloys depends on many factors, i.e., type and amount of grain refiner, alloy compositions, holding time and temperature in the furnace [5, 36, 37].

Dahle et al. [38] reported that the addition of Sr to hypoeutectic Al–Si alloy for eutectic Si modification

delays coherency to higher solid fraction. Çolak et al. [28] also found that Sr modification increases the fluidity of A356 alloy. In contrast, it has been found that the addition of both Sr and Na modifies the eutectic Si and reduces fluidity [10, 39]. In this work, the addition of Sc in Al–Si hypoeutectic alloys can achieve modification of eutectic Si from coarse plate-like morphology to fine fibrous morphology, as shown in Fig. 5d–f. We have found that Sc addition affects the fluidity of the A356 alloys. Both Sc additions at 0.2 and 0.4 wt% improve the fluidity of A356 alloys (Fig. 4).

Pandey et al. [40] reported that the addition of Sc changes the eutectic solidification mode from growth of numerous Si particles near primary Al dendrite tips distributed throughout the sample to growth of a well-defined eutectic front growing from the mold walls opposite to the thermal gradient. High fluidity is generally found to be related to the solidification mechanism, wherein solidification occurs by the plane interface from the mold wall [5]. The solidification of eutectic Si from the mold wall may lead to the higher fluidity length, due to a possible delay in the formation of a coherent network of eutectic.

The Sc added into hypoeutectic Al–Si alloys alter the binary eutectic $L \rightarrow \text{Al} + \text{Si}$ reaction to a ternary eutectic $L \rightarrow \text{Al} + \text{AlSi}_2\text{Sc}_2 + \text{Si}$ reaction [40], as shown in Fig. 6. The Al-rich corner side of the Al–Si–Sc ternary phase diagram is shown in Fig. 11 [32, 40]. The addition of 0.4 wt% Sc leads to more Sc-containing intermetallic phase formation. Moreover, at 0.4 wt% Sc, the Sc-containing intermetallic phase formed in the alloys is AlSi_2Sc_2

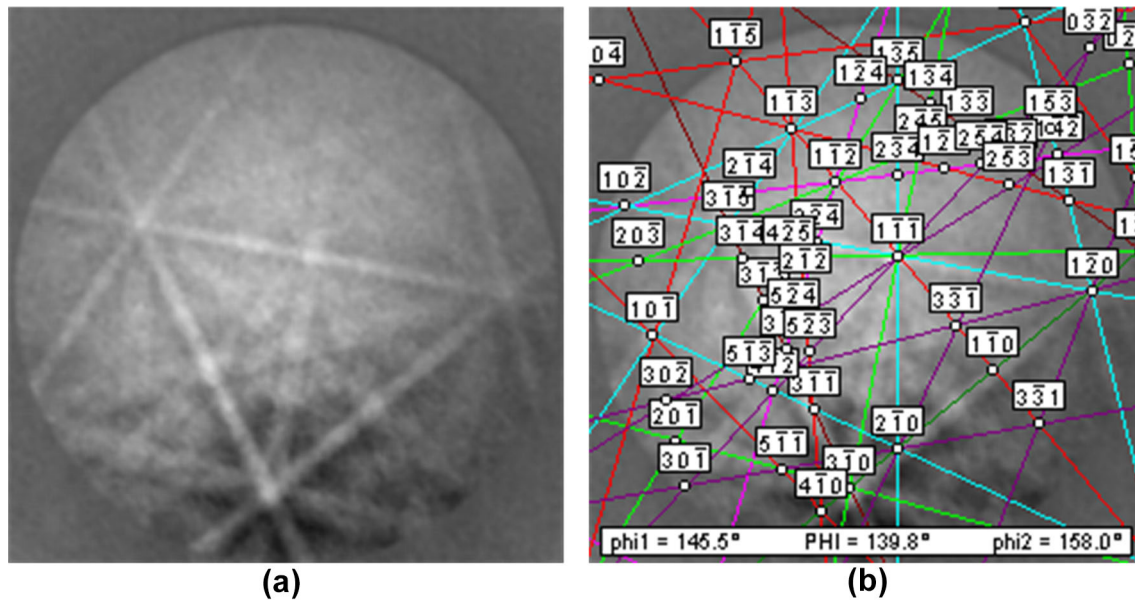


Fig. 9 EBSD patterns: **a** indexed Kikuchi pattern of the AlSi_2Sc_2 phase, and **b** identification of Kikuchi lines

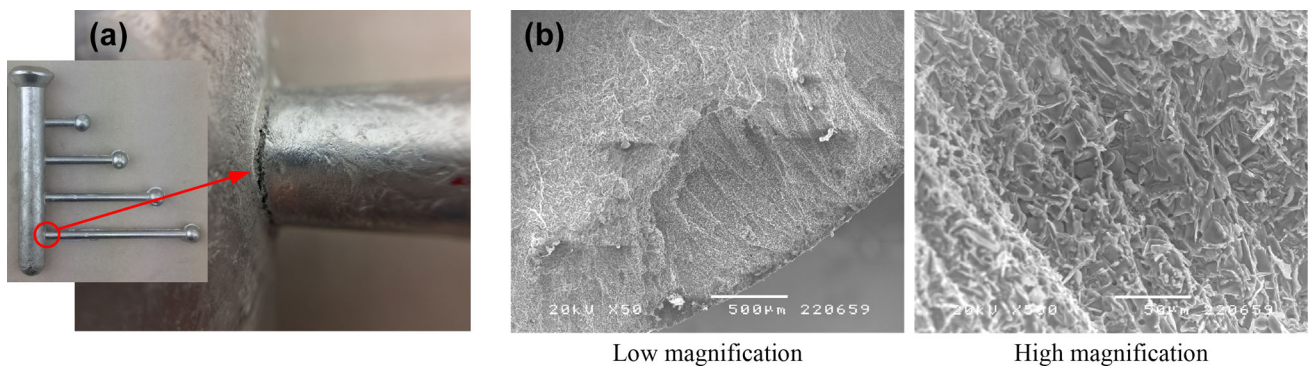


Fig. 10 Hot cracking surfaces of A356 based alloy: **a** macrograph, and **b** SEM micrograph

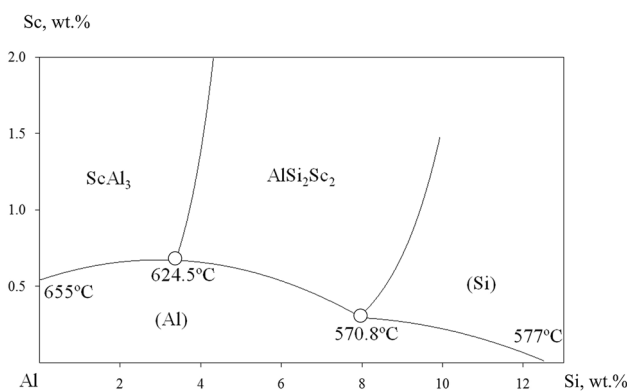


Fig. 11 The Al corner of the Al–Si–Sc phase diagram. Reproduced with permission from Pandey et al. [40]

which grow in the Al– AlSi_2Sc eutectic prior to the main Si-containing eutectic, as shown in Fig. 8. The fluidity of 0.4 wt% Sc alloys slightly decreases, as shown in Fig. 4. It

should be noted that further increasing the Sc addition (at 0.4 wt% Sc) dramatically increases the amount of high melting point AlSi_2Sc intermetallic compounds (Figs. 6, 7, 8). These solid particles are believed to increase the viscosity of the melt and thus decrease the flowability and feeding ability of liquid aluminum. Moreover, AlSi_2Sc_2 intermetallics, which grow in the Al– AlSi_2Sc eutectic, restrict liquid feeding; therefore, the decrease of fluidity in 0.4 wt% Sc alloys is attributed to the presence of large AlSi_2Sc_2 intermetallics.

Figure 12 is a schematic representation of microstructure formation in A356 alloys with and without Sc additions in the fluidity test. During solidification of A356 based alloy, the large dendrites formed in earlier coherency and the numerous Al–Si eutectic grains grow throughout the sample (Fig. 12a); this can lead to problems in the filling of thin sections. In the alloy with 0.2 wt% Sc addition (Fig. 12b), the smaller dendrites formed in later

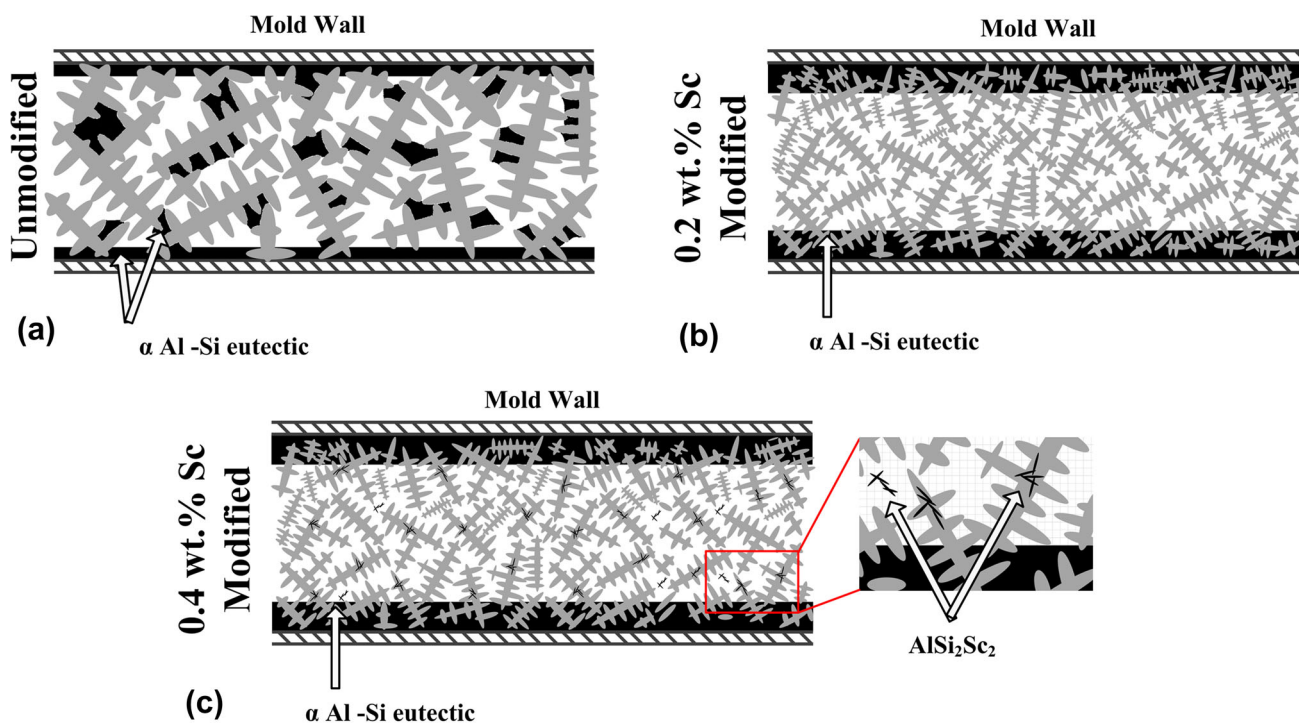


Fig. 12 Schematic illustrations of fluidity at the stage of eutectic solidification: **a** unmodified, **b** 0.2 wt% Sc modified, and **c** 0.4 wt% Sc modified

coherency and the eutectic silicon grow from the mold walls toward the center of the samples. This can improve the fluidity of the alloy; however, the addition of a high level of Sc leads to the formation of large $AlSi_2Sc_2$ intermetallics (Fig. 12c), which can then restrict liquid feeding, thus reducing the fluidity of the alloy.

4.2 Hot Cracking

Hot cracking normally occurs at hot spot areas of castings where the strain resulting from solidification contraction is concentrated and the contraction of a solidifying casting is restrained by the mold. The influencing factors on hot cracking are very complex and many mechanisms have been proposed [4, 41]. Generally, grain refining is a major practice for reducing the hot crack susceptibility. The grain refinement reduces segregation, and thus decreases the effective freezing temperature range and the hot cracking tendency [42]. It is well accepted that the coherency temperature range between the dendrite coherency point and the end of solidification is closely related to hot tearing, i.e., a small coherency temperature range reduces hot cracking susceptibility [4]. In this work, we have found that the addition of Sc results in a remarkable refinement of grains, especially the occurrence of columnar equiaxed transition. The finer grain structure reduces the effective freezing range, and postpones the grain coherency and consequently enhances the feeding ability of the melt,

which are the key for controlling hot cracking. Thus, hot cracking is not found in the samples with Sc addition.

Sr modifier has been reported to increase the HCS of aluminum alloy, due to the formation of strontium oxide particles, which may act as hot cracking crack initiators [43]. Knuutinen et al. [44] reported that the addition of Ca modifier reduces the hot cracking of Al–Si casting alloy. Nogita et al. [45] suggested that the modification of eutectic Si with Ca causes the solidification of eutectic to evolve from the surface of the casting towards the center of the sample. Such an eutectic solidification mode is expected to reduce the hot cracking of the alloy. The solidification of eutectic with Ca addition has a very similar behavior to that of Sc addition. Sc modifies the eutectic Si by changing the solidification mode from numerous Si particles near primary Al dendrite tips to growth from the mold walls, which improves the feeding ability of the alloy resulting in reduced hot cracking susceptibility of the alloy.

Figure 13 is a schematic representation of microstructure formation in A356 alloys with and without Sc additions in CRC mold. During solidification of A356 based alloy, the numerous Al–Si eutectic grains grow throughout the sample (Fig. 13a). In alloy with Sc addition (Fig. 13b), the eutectic silicon grows from the mold walls toward the center of the samples, which may reduce the hot cracking of the A356 alloy.

The results show that hot cracking susceptibility indexes of A356 slightly increases with increasing pouring

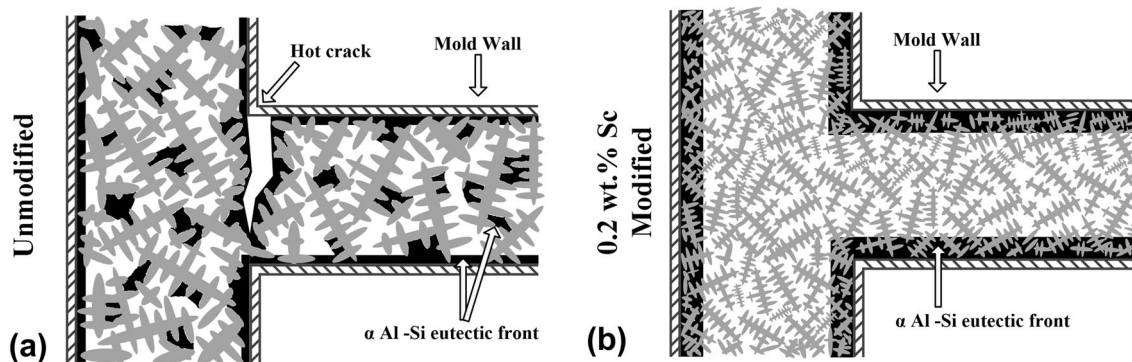


Fig. 13 Schematic illustrations of hot cracking at the stage of eutectic solidification: **a** unmodified, and **b** 0.2 wt% Sc modified

temperature. The effect of pouring temperature or superheat temperature on hot cracking has been previously reported. Li et al. [46] showed that the hot cracking in Al–Cu alloy increases with increasing pouring temperature. The similar results in Mg alloys are also observed [47]. Two mechanisms may be used to explain the increasing hot cracking with increased pouring temperature [46, 47]. First, the melt solidifies with a lower cooling rate; then the grain size becomes larger at an increasing pouring temperature. Subsequently, large grains cause the stress concentration built up. The other possible mechanism is that, the increasing pouring temperature increases the liquid film thickness between grains and thus weakens the coherence among grains, which later leads to higher possibility for hot cracking.

5 Conclusions

The castability of A356 alloys with Sc additions was investigated. The α -Al grain refinement and the modification of eutectic Si morphology from coarse plate-like to fine fibrous by the Sc addition also possibly increased the fluidity. The total volume improved approximately 8.66% at 0.2 wt% Sc modification compared with A356 base alloy. However, there was a slight decrease in the fluidity of alloy with 0.4 wt% Sc addition, which was probably due to the formation of a large amount of AlSi_2Sc_2 intermetallic in the Al– AlSi_2Sc_2 eutectic and AlSi_2Sc_2 intermetallic in the Al– AlSi_2Sc_2 –Si eutectic. The hot cracking of the A356 alloy was completely diminished when Sc was added to the alloy. It was suggested that a combined effect of grain refinement and changing of eutectic solidification mode was responsible for the reduction of hot cracking susceptibility.

Acknowledgements Financial support by the National Research University Project of Thailand's Office of the Higher Education Commission, the King Mongkut's University of Technology Thonburi through the "KMUTT 55th Anniversary Commemorative Fund,"

and the Royal Thai Government Scholarship (Ministry of Science and Technology) for Mr. Kongkiat Puparattanapong for his Ph.D. study is acknowledged.

References

1. Arnberg L, and Mo A, *Castability-Fluidity and Hot Tearing*, Metals Handbook, ASM (2008), p 375.
2. Flemings M C, *Solidification Processing*, Wiley Online Library (1974).
3. Davidson C, Viano D, Lu L, and StJohn D, *Int J Cast Met Res* **19** (2006) 59.
4. Eskin D, and Katgerman L, *Metall Mater Trans A* **38** (2007) 1511.
5. Ravi K R, Pillai R M, Amaranathan K R, Pai B C, and Chakraborty M, *J Alloys Compd* **456** (2008) 201.
6. Kwon Y-D, and Lee Z-H, *Mater Sci Eng A* **360** (2003) 372.
7. Dahle A K, Tøndel P A, Paradies C J, and Arnberg L, *Metall Mater Trans A* **27** (1996) 2305.
8. Loper C Jr, *AFS Trans* **47** (1992) 533.
9. Mollard F, Flemings M, and Niyama E, *AFS Trans* **95** (1987) 647.
10. Kotte B, *Modern Cast.* **75** (1985) 33.
11. Pan E, and Hu J, *Trans Am Foundrym Soc* **105** (1997) 413.
12. Argo D, and Gruzleski J, *Int J Cast Met Res* **2** (1989) 109.
13. Easton M, Wang H, Grandfield J, St John D, and E. Sweet, *Mater Forum* **28** (2004) 224.
14. Rosenberg R, Flemings M, and Taylor H, *Trans Am Foundrym Soc* **68** (1960) 518.
15. Warrington D, and McCartney D, *Int J Cast Met Res* **3** (1990) 202.
16. Gruzleski J, and Closset B, *The Treatment of Liquid Aluminum-Silicon Alloy*, American Foundrymen's Society, Inc. (1990).
17. Robles-Hernandez F C, Ramirez J M H, and Mackay R, *Al-Si Alloys: Automotive, Aeronautical, and Aerospace Applications*, Springer (2017).
18. Patakham U, Kajornchaiyakul J, and Limmaneevichitr C, *J Alloys Compd* **542** (2012) 177.
19. Xu C, Xiao W, Hanada S, Yamagata H, and Ma C, *Mater Charact* **110** (2015) 160.
20. Muhammad A, Xu C, Xuejiao W, Hanada S, Yamagata H, Hao L, and M. Chaoli, *Mater Sci Eng A* **604** (2014) 122.
21. Pandee P, Gourlay C M, Belyakov S A, Patakham U, Zeng G, and Limmaneevichitr C, *J. Alloys Compd* **731** (2018) 1159.
22. Patakham U, Kajornchaiyakul J, and Limmaneevichitr C, *J Alloys Compd* **575** (2013) 273.

23. Prukkanon W, Srisukhumbowornchai N, and Limmaneevichitr C, *J Alloys Compd* **477** (2009) 454.
24. Patakham U, and Limmaneevichitr C, *J Alloys Compd* **616** (2014) 198.
25. Puparattanapong K, and Limmaneevichitr C, *Trans Indian Inst Met* **69** (2016) 1587.
26. Prukkanon W, Srisukhumbowornchai N, and Limmaneevichitr C, *J Alloys Compd* **487** (2009) 453.
27. Di Sabatino M, Shankar S, Apelian D, and Arnberg L, *Influence of Temperature and Alloying Elements on Fluidity of Al–Si Alloys*, in TMS Shape Casting - The John Campbell Symposium (2005), p 193.
28. Çolak M, Kayikci R, and Dispinar D, *Trans Indian Inst Met* **68** (2015) 275.
29. Pekguleryuz M, Labelle P, Argo D, and Baril E, *Magnesium Diecasting Alloy AJ 62 X with Superior Creep Resistance, Ductility and Diecastability*, in Magnesium Technology 2003 as held at the 2003 TMS Annual Meeting (2003), p 201.
30. Cao G, and Kou S, *Mater Sci Eng A* **417** (2006) 230.
31. Toropova L S, Eskin D G, Kharakterova M L, and Dobatkina T V, *Advance Aluminum Alloys containing Scandium: Structure and Properties*, Gordon and Breach Science, Amsterdam (1998).
32. Rokhlin L L, Bochvar N R, Rybal'chenko O V, Tarytina I E, and Sukhanov A V, *Russ Metall* **2012** (2012) 606.
33. Tyvanchuk A T, Yanson T I, and Kotur B, *Russ Metall* **20** (1988) 190.
34. Backerud L, Chai G, and Tamminen J, *Solidification Characteristics of Aluminum Alloys. Vol. 2.*, Foundry alloys, American Foundrymen's Society, Inc. (1990) p 266.
35. Malekan M, and Shabestari S, *Metall Mater Trans A* **40** (2009) 3196.
36. Schumacher P, Greer A L, Worth J, Evans P V, Kearns M A, Fisher P, and Green A H, *Mater Sci Technol* **14** (1998) 394.
37. Greer A L, Bunn A M, Tronche A, Evans P V, and Bristow D J, *Acta Mater* **48** (2000) 2823.
38. Dahle A, Arnberg L, and Apelian D, *Trans Am Foundry Soc* **105** (1997) 963.
39. Venkateswaran S, Mallya R, and Seshadri M, *Trans Am Foundry Soc* **94** (1986) 701.
40. Pandee P, Gourlay C M, Belyakov S A, Ozaki R, Yasuda H, and Limmaneevichitr C, *Metall Mater Trans A* **45** (2014) 4549.
41. Di Sabatino M, and Arnberg L, *Trans Indian Inst Met* **62** (2009) 321.
42. Ram G J, Mitra T, Shankar V, and Sundaresan S, *J Mater Process Technol* **142** (2003) 174.
43. Nabawy A M, Samuel A M, Samuel F H, and Doty H W, *J Mater Sci* **47** (2012) 4146.
44. Knuutinen A, Nogita K, McDonald S D, and Dahle A K, *J Light Met* **1** (2001) 241.
45. Nogita K, Knuutinen A, McDonald S D, and Dahle A K, *J. Light Met* **1** (2001) 219.
46. Li S, Sadayappan K, and Apelian D, *Metall Mater Trans B* **47** (2016) 2979.
47. Huang H, Fu P-h, Wang Y-x, Peng L-m, and Jiang H-y, *Trans Nonferrous Met Soc China* **24** (2014) 922.